7^{th} International Conference on Heat Transfer,
Fluid Mechanics and Thermodynamics,
19 - 21 July 2010, Antalya, Turkey

An expermintal investigation of thermal effects during discharging operations in a hydrogen cryo-adsorption storage system

Petar Aleksić,* Erling Næss, and Ulrich Bunger
Norwegian University of Science and Technology
Department of Process and Energy Engineering
Kolbjørn Hejes vei 1a, NO-7491, Norway
(Dated: January 4, 2010)

Experimental analysis of thermal effects during discharging of a ten liter hydrogen cryo-adsorption storage tank have been performed. Experiments has been conducted with two adsorbent classes: activated carbon and metal-organic-framework. The study was carried out in a cylindrical tank with granular adsorbents in which the bed temperature was measured at various positions. Thermal effects have been investigated as a consequence of variations in the mass out-flows rate and the initial storage pressure. The experiments tried to reproduce scenarios of a hydrogen-fueled powertrain in operation by delivering power input required for a conventional scooter (6 kW) and a fuel-cell vehicle (20 kW). The penalties in quantities of residual gas were reported and suggestions for improvements of thermal management during discharging operations were suggested.

Keywords: hydrogen storage, cryo-adsorption, activated carbon, metal-organic-frameworks

I. INTRODUCTION

If the promises risen from hydrogen-fueled fuel-cell vehicles are to be fullfiled, a number of breakthroughs related to the development of hydrogen storage infrastructure and operation procedures need to be achieved. The DoE and stakeholders within the automobile industry advocate that hydrogen-fueled vehicles need to be able to match the performances of common hydrocarbon fueled powertrains in terms of driving characteristics, safety and cost. Such approach led them to impose a series of targets which present a serious challenge to the developers of hydrogen storage systems [1]. These targets define hydrogen content per unit mass and unit volume, limited energy loss during filling and discharging operations, fast kinetics during charging, high cycle life, minimized cost of recycling and auxiliary equipment and safety concerns in regular service and/or accidents. For the time being, none of the currently investigated storage technologies is able to meet all the criteria at once.

Unlike gasoline or diesel, easily handled under the ambient conditions, hydrogen needs an extra processing to meet gravimetric and volumetric energies densities recommended for on-board storage by the automobile industry. The four major storage technologies for on-board storage systems include: physical storage via compression, hydrogen liquefaction, chemical storage via metal hydrides and gas physisorption on solid adsorbents.

*Electronic address: petar.aleksic@ntnu.no

Hydrogen storage via adsorption has probably received the least research attentions due to the controversial reports of hydrogen uptake reported which later failed to be reproduced [2]. Recently, more consistent results have been reported and confirmed by different research groups with more consistent sample preparation, activation procedures and measuring techniques. Gas physisorption offers fast kinetics of charging and discharging as hydrogen is maintained in molecular identity. Furthermore, this arrangement could potentially offer a reduction of the storage pressure. While the above mentioned characteristics are favorable to physisorption, reported hydrogen uptakes on carbon materials and metal-organic-frameworks do not exceed $2wt\%$ at room temperature [3]. Due to such moderate adsorption potential exhibited at near ambient temperatures, the adsorption type storage systems need to be operated at the temperatures close to the temperature of liquid nitrogen (LN2). Such storage system consists of a cryogenic vessel packed with an adsorbent and auxiliary equipment required for the maintaining the low temperature. Liquid nitrogen is attractive due the low cost and wide availability.

Reaching gravimetric and volumetric targets for on-board storage systems suggested by the DoE have been marked by scientific community as crucial enabling factors for commercialization of hydrogen-fuelled powertrains [4]. Improvements in the volumetric and gravimetric storage capacity for all relevant storage technologies in the last decade have been reported [5–7]. Currently, maximum hydrogen uptake of 5.8 wt% on carbon materials and 7.5 wt% on metal-organic-framework (MOF) at 77 K has been reported [8]. Apart from the mate-

rial development, thermal effects that occur during high-pressure charge and discharge operations in adsorption type storage systems can seriously hinder the storage capacity of the system during the re-filling and cause significant amount of residual gas trapped in the tank during discharging [9, 10]. Lamari et al. [11] have investigated dynamics of re-filling and discharging processes of a hydrogen storage system at near ambient temperatures and high pressures. At the analyzed operational conditions, the amount of adsorbed hydrogen is quite moderate. In this paper, we focused on thermal effects during discharging of a hydrogen cryo-adsorption system, combining optimal operating conditions i.e. moderately high pressure (up to 2 MPa) and low temperature for gas storage process purpose. The experimental analysis is conducted with two adsorbent classes: activated carbon (AC) and metal-organic-frameworks (MOF).

II. EXPERIMENTAL SETUP

Experimental setup is designed and built to enable investigation of thermal effects in a cryo-adsorption storage system during charging and discharging operations with diverse pelletized adsorbents. The experimental setup consists of two main lines: charge and discharge. Figure 1 displays a simplified layout of the discharge line. The main components of the discharge line are: adsorption column, gas-handling and measuring equipment and data-acquisition system. The adsorption column (1) is a stainless-steel cylinder with internal and external diameters of 132 mm and 135 mm, respectively. The internal length of the column is 720 mm and the total internal volume is $9.853{\cdot}10^{-3}$ m^3. Twelve thermocouples of type T (Txx) are distributed along the column to allow measurement of temperature variations in axial and radial direction during the discharging operations. A digital pressure transducer is mounted on the upper flange of the storage vessel, able to measure pressure up to 6 MPa. The tank is equipped with a release valve (4) to prevent uncontrolled pressure increase in the tank. The column is packed with a palletized adsorbent. The analysis is conducted with a commercially available activated carbon (NORIT R0.8) and metal-organic-framework (Cu-1,3,5-BTC) synthesized in BASF laboratories. The activated carbon adsorbent has specific surface area (SSA) of 1385 m^2/g, bulk density of 400 kg/m^3 and cylindrical shape particles (3×0.8) while the MOF adsorbent measures SSA and bulk density of 1154 m^2/g and 485 kg/m^3, respectively. The storage vessel is emerged in a liquid nitrogen bath (2).

The gas-handling and measurement line consists of: particle filter (3), shut-off valve (5), shell-and-tube heat exchanger (6), pressure regulator (7) and mass flow controller (8). The particle filter serves to prevent eventual penetration of particles in the measuring equipment. The shut-off valve enables start/termination of discharging operations. The heat exchanger is employed to heat up the outflow gas before entering the mass flow controller. The pressure regulator with the reading accuracy of ±3% is used to reduce the gas pressure to a prediscribed value required for feeding of fuel-cells. Hydrogen mass outflow is measured and controlled by use of the mass-flow controller (Brooks Ins.5851S) with the full-scale of 120 nlit/min. The reading accuracy of the flow controller was 0.7 %. The data acquisition system (9) includes a personal computer linked to the thermocouples, the pressure transducer and the mass-flow controller via multifunction consoles (NI cFP). The mass-flow rate is governed by a Brooks Ins power/control unit (Brooks Ins. 0154). The data were recorded by use of LabView software application. The acquisition frequnecies for the temperature, pressure and flow variations were 0.5 s.

Experiments were carried out with the initial pressure in the tank of 2 MPa. Before the discharging of the storage tank, the mean temperature in the bed was adjusted to 81 K with maximum temperature variation of 1 K. Commence of discharging was initiated by opening of the shut-off valve (5). At the given parameters, 142.9 g of hydrogen was stored in the tank. Downstream from the valve, the pressure regulator was used to allow gas expansion to 0.25 MPa. The constant flow rate, that determines the available power, varied between 0.05 g/s and 0.12 g/s. Such mass flow provide power required of 6 kW (scooter) and 15 kW (small city electrical vehicle). When the pressure in the tank reached the 0.25 MPa, the shut-off valve was used to terminate the outflow of hydrogen.

III. RESULTS AND DISCUSSION

The thermal behavior and its influence on the performance of the proposed storage system is analyzed with respect to variations of: adsorbent's class and discharging mass rate.

Since it is not possible to represent the vast amount of experimental data obtained at twelve measuring positions, only positions of thermocouples significant for the analysis are presented at figure 2. Thermocouple T1 is placed on the axis close to the outlet of gas. Thermal sensor T2 lies on the axis and 205 mm from the upper flange. Thermocouples T3, T4 and T5 are positioned in the middle section of the storage column. Thermocouple T3 lies in the center, T5 is placed in the vicinity of the vertical wall and T4 is positioned on the midway between thermal sensors T3 and T5. Thermocouple T6 is placed on the vertical axis and close to the bottom of the tank.

Figures 3 and 4 display gas flow and pressure histories for the initial pressure of 2 MPa and gas outflows of 0.05 g/s for the activated carbon and the MOF adsorbent, respectively. Two distinctive region could be observed from the graphs. The first region is characterized with the constant outflow rate, and gradual pressure decrease. In the moment when the pressure in the tank reaches 0.25 MPa, shut-off valve is used to terminate the outflow. In the sec-

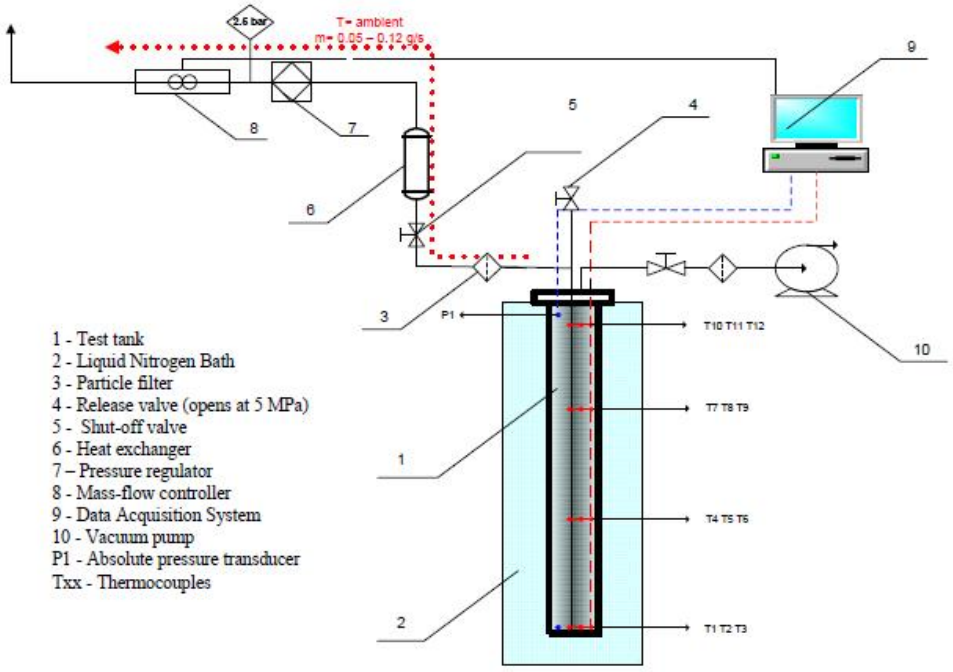

FIG. 1: Layout of the experimental setup used for investigation of dynamical thermal behavior of storage system during discharging

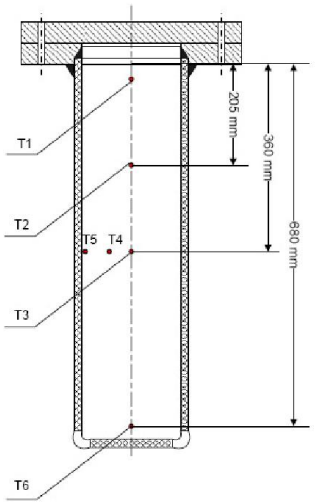

FIG. 2: Positions of thermocouples in storage tank

ond region, a pressure increase in the tank is observed as a consequence of temperature increase and redistribution of quantities of adsorbed gas and gas stored in voids of the bed. It could be noted that the column filled with the MOF adsorbent allows extended discharging time (1225 s comparing to 1036 s for the activated carbon system).

Figures 5 and 6 show typical temperature histories at different radial and axial positions. As expected, a temperature decline was observed in all measuring points. The temperature decrease is influenced by decompression and desorption. It could be noted that during the first phase, all temperature measuring points placed in the core of the tank recorded identical temperature drop. An average temperature drop in the core of the bed of 13.55 K and 13.45 K at the end of discharging phase were recorded for the activated carbon and the MOF adsorbent, respectively. Temperature decent recorded in the vicinity of the wall (T5) was considerably lower than for the remaining part of the column. Influence of the heat penetration from the column's surrounding was observed only in the region situated in the areas close to the walls. At the end of discharge, an average temperature drop recorded in the vicinity of the wall was 4.1 K. Such observation leads to conclusion that problems of discharging could be sufficiently analyzed as a one-dimensional radial model. After the period of the gas release, the temperature in the tank gradually increased. During the observed timespan, the complete temperature recovery for the both analyzed scenarios was only observed in the region close to the walls of the column. The temperature sensors positioned in the core of the column recorded an average temperature recovery of 7.2 K for the activated carbon and 4.1 K for the MOF adsorbent.

Figures 7 and 8 display calculated variations of the hy-

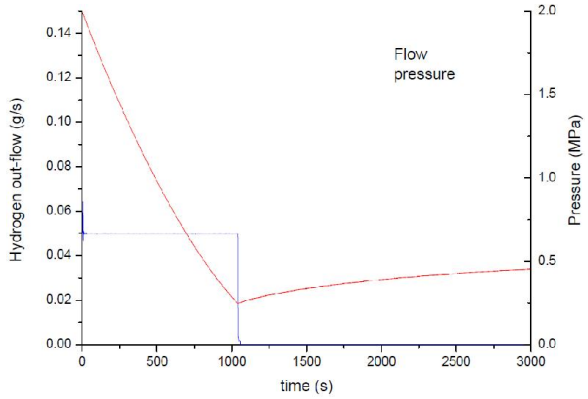

FIG. 3: Measured mass flow and pressure histories recorded during discharging from 2 to 0.25 MPa for the AC adsorbent. Outflow 0.05g/s

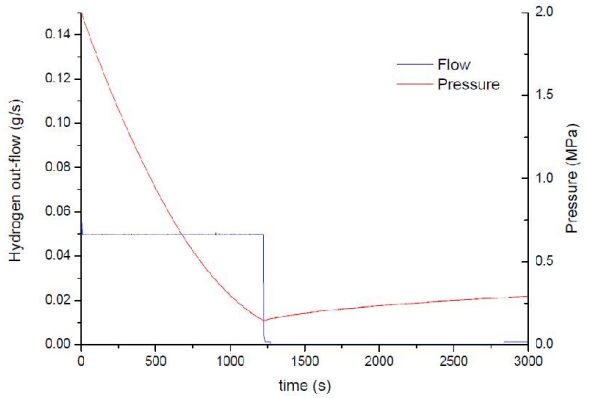

FIG. 4: Measured mass flow and pressure histories recorded during discharging from 2 to 0.25 MPa for the MOF adsorbent. Outflow 0.05g/s

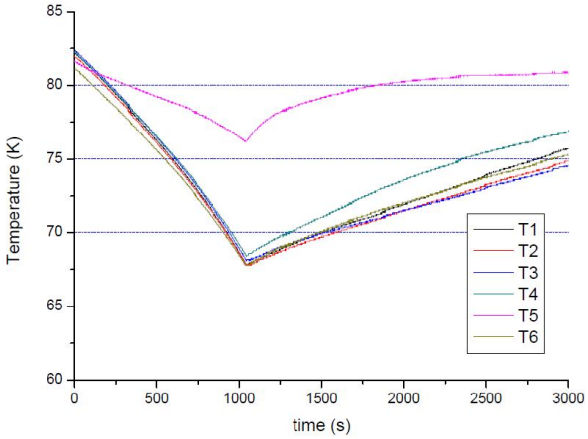

FIG. 5: Measured temperature histories at various positions in the tank for AC adsorbent. Corresponds to discharging conditions shown in Fig. 3

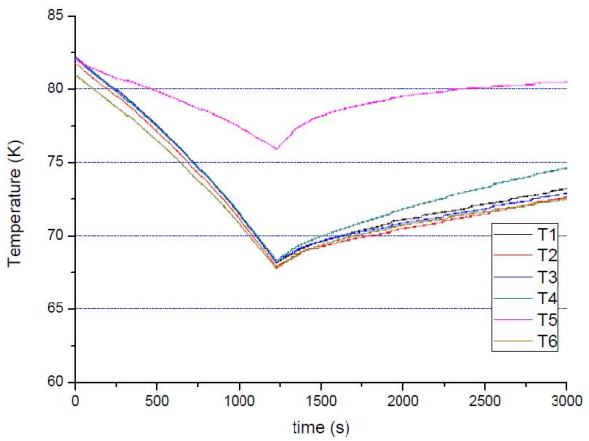

FIG. 6: Measured temperature histories at various positions in the tank for MOF adsorbent. Corresponds to discharging conditions shown in Fig. 4

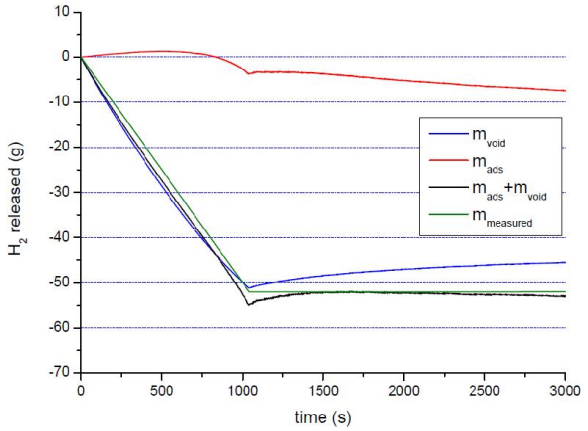

FIG. 7: Calculated amounts of hydrogen adsorbed (m_{ads}) and stored in the voids (m_{void}) of the tank during discharging and measured hydrogen outflow ($m_{measured}$). Corresponds to experiments shown in Fig. 3

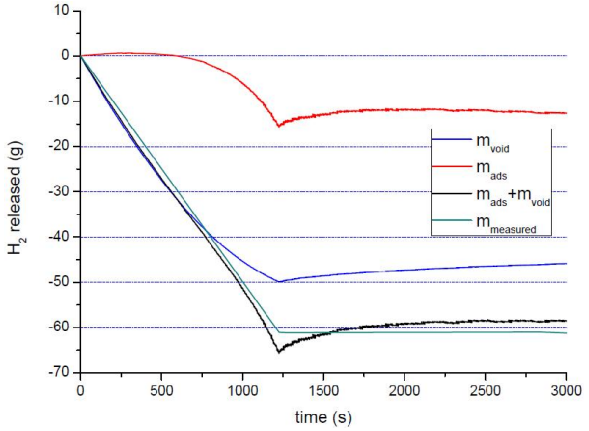

FIG. 8: Calculated amounts of hydrogen adsorbed (m_{ads}) and stored in the voids (m_{void}) of the tank during discharging and measured hydrogen outflow ($m_{measured}$). Corresponds to experiments shown in Fig. 4

drogen stored in the voids and hydrogen adsorbed during the discharging of the tank for the activated carbon and MOF adsorbent, respectively. The mass outflow ($\dot{m}_{out}$) is a sum of desorption and decompression rates:

$$\dot{m}_{out} = \frac{dm_{void}(p,T)}{dt} + \frac{dm_{des}(p,T)}{dt}$$

[amout]$\dot{m}_{out}$Mass outflow (g/s) [ades]m_{des}Quantity of adsorbed hydrogen (g) [amvoid]m_{void}Mass of hydrogen stored in voids (g) [at]$t$time (s) [ammeasured]$m_{measured}$Hydrogen outflow measured experimentally (g)

The quantity of adsorbed hydrogen (m_{des}) is calculated by use of the Langmuir model fitted according to the measured adsorption isotherms [12]. The quantity of hydrogen stored in the voids (m_{void}) of the column is estimated by use of the ideal gas law. As shown in figures 7 and 8, the proposed model has showed a good accordance with the hydrogen outflow measured experimentally ($m_{measured}$). It could be noted that during the period of the gas outflow the majority of the gas is released from the voids of the column. In the higher pressure region, when the adsorption isotherms are more sensitive to temperature than pressure variations, the quantity of adsorbed hydrogen increased due to the temperature decline. Only towards the end of the gas discharging, at the lowered pressure, a decrease in the amount of adsorbed hydrogen in the column is observed. The higher thermal mass of the MOF adsorbent, resulted with and increase of desorbed hydrogen during the discharging. After the termination of discharging, as a consequence of temperature recovery, a further decrease in the amount of adsorbed hydrogen is recorded. The penalties in the amount of the residual gas is estimated to 62.2 % for the activated carbon and 59.8 % for the MOF adsorbent.

The influence of mass outflow has been examined for the storage system packed with the activated carbon. Figure 9a displays pressure and flow histories for the initial pressure in the tank of 2 MPa. The outflow of 0.05 g/s and 0.12 g/s has given discharging times of 1036 s and 431 s, respectively. Figure 9b shows temperature variations recorded in the middle section of the column (positions T3 and T5) for gas outflows of 0.05 g/s and 0.12 g/s. It could be observed that the equal temperature drop at the measured positions is recorded regardless of the outflow variations. The maximum temperature drop of 13.55 K at the position T3 and 5.11 K at the position T5 are recorded. In the second regime, when the outflow is terminated, the thermocouple place in the vicinity of the wall recorded a full temperature recovery is observed within 1500 s. During the observed timespan an average temperature recovery rate of $3.8{\cdot}10^{-3}$ K/s was measured.

Presented graphs allow us to draw two major conclusions:

- heat source is necessary in order to avoid the vast penalty in the residual gas

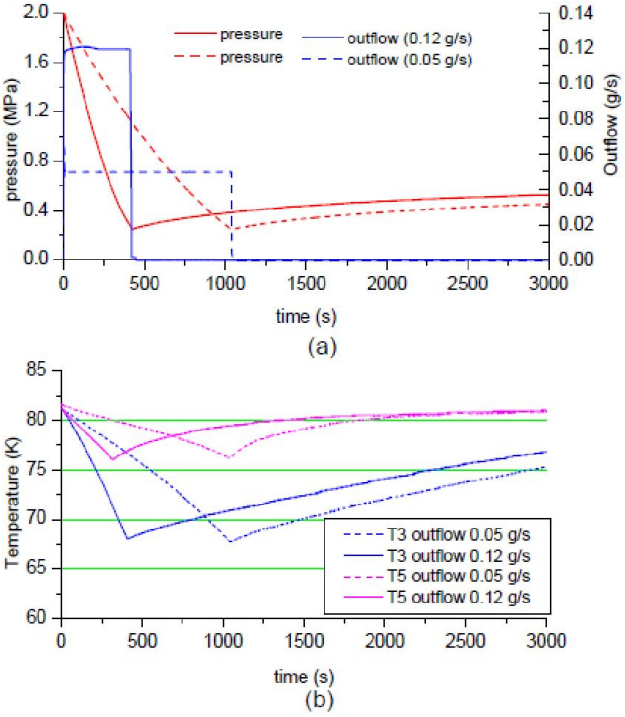

FIG. 9: Measured pressure and outflow (a) and temperature histories (b) AC adsorbent with the discharge rate 0.05 g/s (dotted line) and 0.12 g/s (solid line). Initial pressure 2 MPa

- low effective thermal conductivity of the bed limits the heat penetration from the outer walls

Almost identical temperature decline, regardless of the outflow variations, point out to low effective thermal conductivity of the bed. Several publications have pointed out that limitations in thermal conductivity could seriously reduce the re-filling and discharging dynamics of adsorption-type storage systems [13–15]. An experimental analysis was performed to estimate the effective thermal conductivity of the adsorption column. A guarded hot plate apparatus was used for the determination of thermal conductivities for the both adsorbents. The apparatus is capable to measure thermal conductivities over the wide temperature range (from 150 to 300 K) and pressure range from vacuum to 0.2 MPa in steady-state conditions [16, 17]. The analysis has been conducted with inert gases (helium and argon). The results were later used to develop a model for the thermal conductivity of a hydrogen-adsorbent system. The estimated thermal conductivity for the temperature range from 80 to 150 K for the activated carbon varies from 0.15 to 0.2 $\frac{W}{mK}$.

The limited hydrogen desorption rate during the discharging showed that the that vast amount of hydrogen gas remained adsorbed in the tank. Such findings point out to the necessity of a controlled heat input during discharging which will ensure that the remaining gas will be delivered to fuel-cells. In order to extend the “driving

time", two scenarios have been analyzed in the following section.

IV. IMPROVEMENTS IN OPERATION OF A CRYO-ADSORPTION STORAGE SYSTEM

Figure 10 displays schematic of two scenarios for the improved thermal management during discharging of the analyzed storage tank. In the first scenario, it is assumed that the storage system initially operates under the isothermal conditions. After the pressure in the tank decreases to 0.25 MPa, heat is supplied to maintain the desired gas outflow (0.05 g/s). Also in the second investigated scenario, two regions could be distinguished. In the first region, the system operates under isobaric conditions and the hydrogen outflow is maintained by the heat input. During the second stage, the gas is expanded under the isothermal conditions.

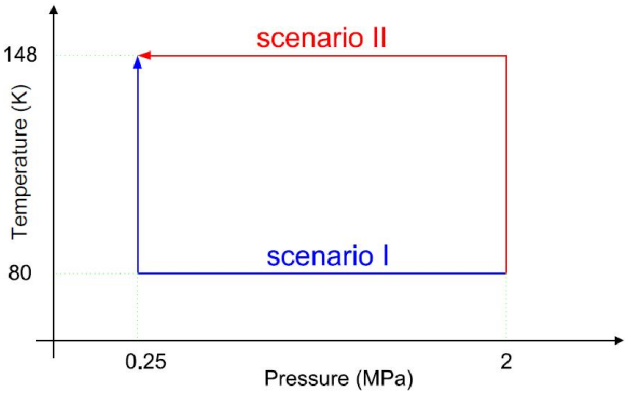

FIG. 10: Considered scenarios for improvement of thermal behavior during discharging

Scenario I: Figure 11 presents pressure and temperature profiles during the discharging operations. During the first stage, the pressure in the tank decreases from 2 MPa to 0.25 MPa in 1480 s. During the second stage, the storage system operates at the constant pressure (0.25 MPa) and heat is invested in the tank to enhance hydrogen desorption. Figure 12 displays redistribution in the amount of adsorbed hydrogen and hydrogen stored in the void of the storage column. In the first stage, when the tank operates under the isothermal conditions, the majority of gas, required to maintain the constant outflow, comes from the hydrogen stored in the voids. In the lower pressure region (below 0.5 MPa), the portion of desorbed hydrogen in the outflow increases. At the end of the isothermal expansion , only 8.2 % of adsorbed hydrogen is discharged. With the heat input, applied during the isobaric heating phase, hydrogen desorption becomes more pronounced. Increasing temperature to 200 K would prolong the driving time and deplete the total amount of hydrogen from the storage tank in 2500

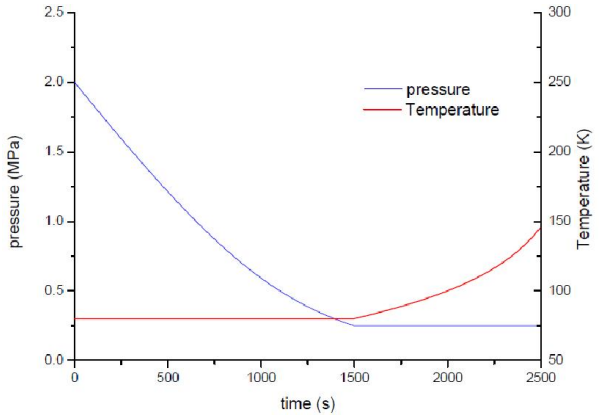

FIG. 11: Pressure and temperature development during discharging scenario I from 2 to 0.25 MPa for activated carbon adsorbent. Outflow rate 0.05 g/s

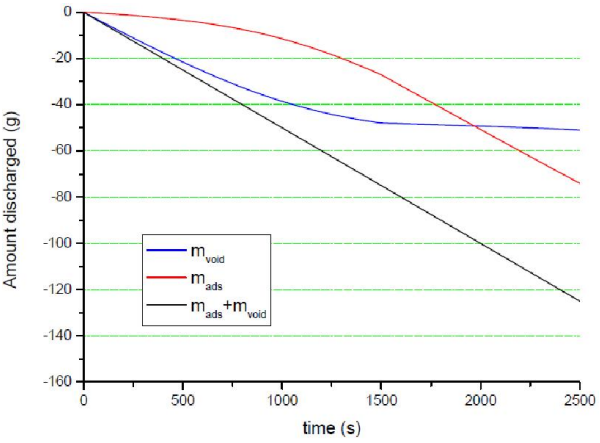

FIG. 12: Calculated contributions from desorbed and hydrogen stored in voids during discharging scenario I. Discharge rate: 0.05 g/s

s. However temperature increase in the bed for on-board storage systems is limited with the available heat from the fuel cells. Assuming the efficiency of 60 % for fuel-cells [18], the following heat balance is derived:

$$\left[\epsilon \cdot \rho_{H_2} \cdot c_{p_{H_2}} + (1-\epsilon) \cdot \rho_{solid} \cdot c_{p_{solid}}\right] \cdot V_{tank} \cdot \frac{dT}{dt} = \dot{m}_{out} \cdot LHV \cdot 0.4$$

[grhoh2]ρ_{H_2}Hydrogen density (kg/m^3) [acph2]$c_{p_{H_2}}$Heat capacity of hydrogen $(J/(g \cdot K))$ [gepsilon]ϵPorosity (-) [grhosolid]ρ_{solid}Adsorbent density (kg/m^3) [acph2]c_{solid}Heat capacity of adsorbent $(J/(g \cdot K))$ [aVtank]V_{tank}Tank volume (m^3) [aT]TTemperature(K) [aLHV]LHVLower heating value of hydrogen (J/g)

where m_{H_2} and m_{solid} are the mass of the gas and the mass of the adsorbent in the tank, respectively. $c_{p_{H_2}}$

denotes specific heat capacity of hydrogen, while $c_{p_{solid}}$ stand for specific heat capacity of adsorbent. Lower heating value of hydrogen is denoted with LHV and porosity with ϵ. The gas outflow is $\dot{m}_{out}$. The maximum feasible temperature increase is limited to 148 K. For the given temperature, the penalty in the residual hydrogen is reduced to 7.54 %.

Scenario II: Calculated pressure and temperature profiles for the scenario II are given in figure 13. While the temperature increases from 80 K to 148 K in 1475 s at the constant pressure (2 MPa), the quantities of both adsorbed and hydrogen stored in the voids decrease. At the end of the isobaric heating, 56 % of the adsorbed hydrogen is depleted (Figure 14). During the period of isothermal decopression, the rate of hydrogen desoprtion decreases. At the end of the discharging period, the penalty in the amount of residual adsorbed hydrogen is 13.38%.

Heat input in the analyzed scenarios sums the heat invested for heating the solid adsorbent and the gas stored in the voids, heat required to compensate heat used for hydrogen desorption and heat consumed during the gas decompression. The heat balance is presented below:

$$Q = (1-\epsilon)\cdot\rho_{solid}\cdot c_{p_{solid}}\cdot V_{tank}\cdot\frac{dT}{dt} + \\ +\epsilon\cdot(\rho_{void}+\rho_{ads})\cdot c_{p_{H_2}}\cdot V_{tank}\cdot\frac{dT}{dt} + \\ +\frac{dm_{des}}{dt}\cdot\Delta H_{ad} + V_{tank}\cdot\frac{dp}{dt}$$

[adH]ΔH_{ad}Heat of adsorption (J/g) [ap]pPressure in tank (Pa))

Heat that needs to be invested for the gas retrieval for the both scenarios is shown in figure 15. Comparing the heat duties for the analyzed scenarios show that scenario II requires about 20 % more energy than scenario I. The reason for the higher heat duty in the scenario II is due the higher thermal mass during isobaric heating. Calculations performed show that the heat released during hydrogen desorption is responsible for almost 60 % of the total heat duty. However, the total heat that needs to be invested in order to minimize the penalties in the residual gas proposed in the scenarios is less the 3 % of the total energy content of the discharged hydrogen.

V. CONCLUSION

Adsorption is one of the currently investigated technologies for hydrogen on-board storage systems. Fundamental information about the potential of adsorption storage systems are represented by adsorption isotherms. However a operational dynamics of discharging of an adsorption type storage systems strongly depend on thermal conductivity and heat management. A penalty in the residual gas of over 60 % is recorded in the investigated cryo-adsorption storage systems without an adequate heat enhancement and heat input devices.

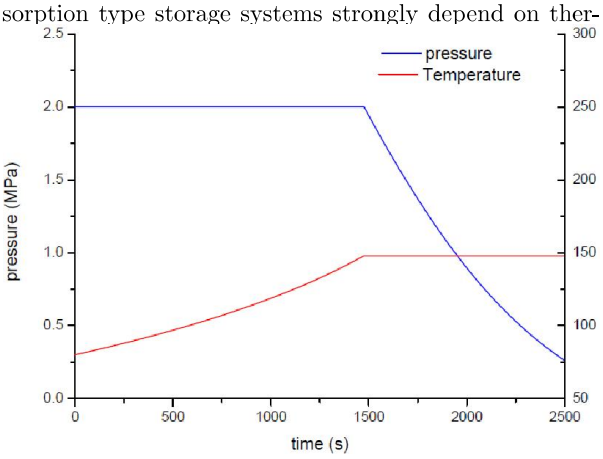

FIG. 13: Pressure and temperature development during discharging scenario II from 2 to 0.25 MPa for activated carbon adsorbent. Outflow rate 0.05 g/s

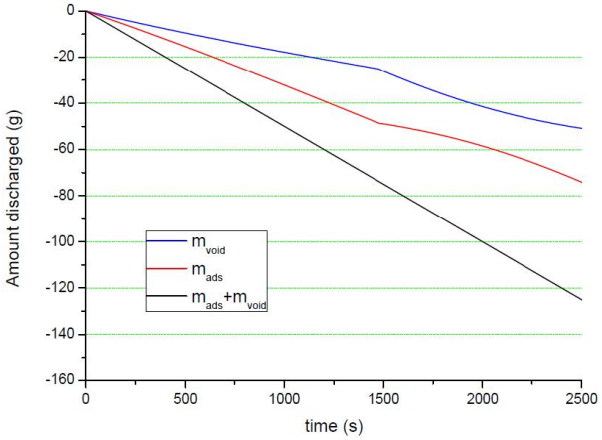

FIG. 14: Calculated contributions from desorbed and hydrogen stored in voids during discharging scenario II. Discharge rate: 0.05 g/s

Analyzed scenarios offer possible improvements by applying a waste heat from fuel-cells to facilitate hydrogen desorption. From the point of feasibility, both scenarios require a small portion in comparison to the energy content of the initially stored hydrogen.

[1] D. Ross, Hydrogen storage: The major technological barrier to the development of hydrogen fuel cell cars, Vacuum 80 (2006) 1084–1089.

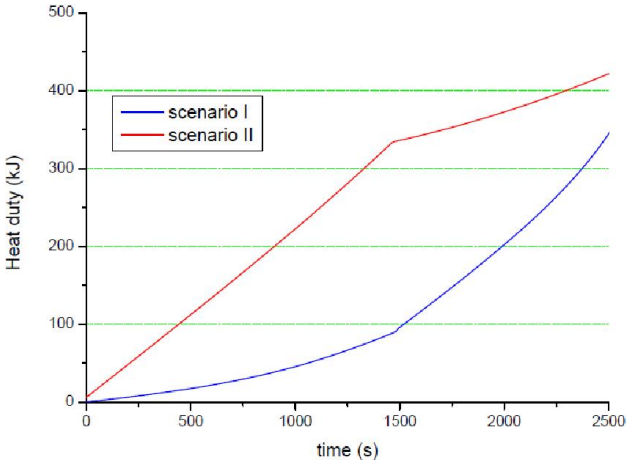

FIG. 15: Required heat input during the discharging for the scenarios I and II

[2] A. C. Dillon, K. M. Jones, T. A. Bekkedahl, C. H. Kiang, D. S. Bethune, M. J. Heben, Storage of hydrogen in single-walled carbon nanotubes, Nature 386 (1997) 377 – 379.

[3] R. Ahluwalia, J. Peng, Automotive hydrogen storage system using cryo-adsorption on activated carbon, Int. J. of Hydrogen Energy 34 (2009) 5476–5487.

[4] D. Mori, K. Hirosea, Recent challenges of hydrogen storage technologies for fuel cell vehicles, Int. J. of Hydrogen Energy 34 (2008) 4569–4574.

[5] E. Tzimas, C. Filou, S. Peteves, J. Veyret, Hydrogen storage: state-of-the-art and future perspective, Website, `http://ie.jrc.ec.europa.eu/publications/scientificpublications/2003/P2003-181=EUR20995EN.pdf` (2003).

[6] L. Zhou, Progress and problems in hydrogen storage methods, Renewable and Sustainable Energy Reviews 9 (2005) 395–408.

[7] M. Conte, P. P. Prosini, S. Passerini, Review of energy/hydrogen storage: state-of-the-art of the technologies and prospects for nanomaterials, Materials Science and Engineering 108 (2004) 2–8.

[8] K. Thomas, Hydrogen adsorption and storage on porous materials, Catalysis today 120 (2006) 389–398.

[9] P. Aleksić, E. Naess, U. Bnger, O. Snju, Experimental analysis of transient thermal behavior in hydrogen cryo-adsorption storage systems, Heat transfer research 40 (2009) 79–89.

[10] P. Aleksić, E. Naess, Experimental study of thermal effects in a hydrogen cryo-adsorption storage system, In Proceedings of ASME 2009: International Mechanical Engineering Congress and Exposition.

[11] M. Lamari, A. Aoufi, P. Malbrunot, Thermal effects in dynamic storage of hydrogen by adsorption, AIChE J 46 (2000) 632–641.

[12] P. Aleksic, E. Naess, U. Buenger, M. Hirscher, M. Schlichtenmayer, Influence of thermal effects during fast filling operations on adsorption capacity in a hydrogen cryo-adsorption storage tank, article in Press (2010).

[13] A. Delahaye, A. Aoufi, A. Gicquel, Improvement of hydrogen storage by adsorption using 2d modeling of heat effects, AIChE Journal 48 (2002) 2061–2073.

[14] G. Momen, G. Hermosilla, M. Pons, K. Firdaouss, K. Hassouni, Hydrogen storage in an activated carbon bed: Effect of energy release on storage capacity of the tank, Int. J. of Hydrogen Energy 34 (2009) 3799–3809.

[15] S. Jensen, E. Nss, Sensitivity analysis of parameters related to the modeling of adsorption-type hydrogen storage tanks, Heat Transfer Research 40 (2009) 143–164.

[16] E. Brendeng, P. Frivik, On the design of a guarded hot plate apparatus, Annexe 1969-7 International Institute of Refrigeration 1969-7 (1969) 281–288.

[17] E. Brendeng, P. Frivik, New development in design of equipment for measuring thermal conductivity and heat flow, Heat Transmission Measurements in Thermal Insulations 544 (1974) 147–166.

[18] U. Bossel, Efficiency of hydrogen fuel cell, diesel-sofc-hybrid and battery electric vehicles, European Fuel Cell Forum.